Transmission of 1.936 Tb/s (11 × 176 Gb/s) DP-16QAM superchannel signals over 640 km SSMF with EDFA only and 300 GHz WSS channel

Jianqiang Li,[1,*] Magnus Karlsson,[2] Peter A. Andrekson,[2] and Kun Xu[1]

[1]*State Key Laboratory of Information Photonics and Optical Communications, Beijing University of Posts and Telecommunications, Beijing, 100876, China*

[2] *Photonics Lab, Department of Microtechnology and Nanoscience, Chalmers University of Technology, 41296, Sweden*

[*]*jianqiangli@bupt.edu.cn*

Abstract: With an improved receiver-side spectral shaping technique by introducing and optimizing one tap coefficient in the intermediate response, we successfully transmitted 1.936 Tb/s (11 × 176 Gb/s) DP-16QAM superchannel signal over 8 × 80 km SSMF with EDFA-only and two 280 GHz wavelength selective switches (WSSs) in support of future 1.6 Tb/s Ethernet with up to 20% forward error correction overhead. The 280 GHz 3-dB bandwidth of the WSS passband permits a sufficient guardband if the 1.936 Tb/s superchannel signals are placed in a 300 GHz WSS channel.

OCIS codes: (060.1660) Coherent communications; (060.2330) Fiber optics communication; (060.4230) Multiplexing.

References and links

1. P. J. Winzer, "Beyond 100G Ethernet," IEEE Commun. Mag. **48**(7), 26–30 (2010).
2. X. Liu, S. Chandrasekhar, B. Zhu, P. J. Winzer, A. H. Gnauck, and D. W. Peckham, "448-Gb/s reduced-guard-interval CO-OFDM transmission over 2000 km of ultra-large-area fiber and five 80-GHz-grid ROADMs," J. Lightwave Technol. **29**(4), 483–490 (2011).
3. Y. Ma, Q. Yang, Y. Tang, S. Chen, and W. Shieh, "1-Tb/s single-channel coherent optical OFDM transmission over 600-km SSMF fiber with subwavelength bandwidth access," Opt. Express **17**(11), 9421–9427 (2009).
4. J. Yu, Z. Dong, X. Xiao, Y. Xia, S. Shi, C. Ge, W. Zhou, N. Chi, and Y. Shao, "Generation of 112 coherent multi-carriers and transmission of 10 Tb/s (112x100Gb/s) single optical OFDM superchannel over 640 km SMF," in Proc. OFC2011, Mar. 2011, Paper PDPA6.
5. G. Bosco, A. Carena, V. Curri, P. Poggiolini, and F. Forghieri, "Performance limits of Nyquist-WDM and CO-OFDM in high-speed PM-QPSK systems," IEEE Photon. Technol. Lett. **22**(15), 1129–1131 (2010).
6. R. Schmogrow, M. Winter, M. Meyer, D. Hillerkuss, S. Wolf, B. Baeuerle, A. Ludwig, B. Nebendahl, S. Ben-Ezra, J. Meyer, M. Dreschmann, M. Huebner, J. Becker, C. Koos, W. Freude, and J. Leuthold, "Real-time Nyquist pulse generation beyond 100 Gbit/s and its relation to OFDM," Opt. Express **20**(1), 317–337 (2012).
7. X. Zhou, L. E. Nelson, P. Magill, R. Isaac, B. Zhu, D. W. Peckham, P. I. Borel, and K. Carlson, "PDM-Nyquist-32QAM for 450-Gb/s per-channel WDM transmission on the 50 GHz ITU-T grid," J. Lightwave Technol. **30**(4), 553–559 (2012).
8. J.-X. Cai, C. R. Davidson, A. Lucero, H. Zhang, D. G. Foursa, O. V. Sinkin, W. W. Patterson, A. N. Pilipetskii, G. Mohs, and N. S. Bergano, "20 Tbit/s transmission over 6860 km with sub-Nyquist channel spacing," J. Lightwave Technol. **30**(4), 651–657 (2012).
9. C. Cole, "Beyond 100G client optics," IEEE Commun. Mag. **20**(2), S58–S66 (2012).
10. J. Li, E. Tipsuwannakul, M. Karlsson, and P. A. Andrekson, "Low-complexity duobinary signaling and detection for sensitivity improvement in Nyquist-WDM coherent system," presented in OFC2012, LA, CA, Mar. 2012, Paper OM3H.2.
11. J. Li, E. Tipsuwannakul, T. Eriksson, M. Karlsson, and P. A. Andrekson, "Approaching Nyquist limit in WDM systems by low-complexity receiver-side duobinary shaping," J. Lightwave Technol. **30**(11), 1664–1676 (2012).
12. J. Yu, Z. Dong, H. -C. Chien, Z. Jia, D. Huo, H. Yi, M. Li, Z. Ren, N. Lu, L. Xie, K. Liu, X. Zhang, Y. Xia, Y. Cai, M. Gunkel, P. Wagner, H. Mayer, and A. Schippel, "Field trial Nyquist-WDM transmission of 8×216.4Gb/s PDM-CSRZ-QPSK exceeding 4b/s/Hz spectral efficiency," in Proc. OFC2012, Los Angeles, CA, Mar. 2012, post-deadline paper PDP5D.3.
13. H.-C. Chien, J. Yu, Z. Jia, Z. Dong, and X. Xiao, "Performance assessment of noise-suppressed Nyquist-WDM for terabit superchannel transmission," to be published in J. Lightwave Technol.

#177331 - $15.00 USD Received 1 Oct 2012; revised 11 Nov 2012; accepted 11 Nov 2012; published 29 Nov 2012

14. J. Yu, Z. Dong, H.-C. Chien, Z. Jia, X. Li, and N. Chi, "WDM transmission of 108.4-Gbaud PDM-QPSK signals (40×433.6-Gb/s) over 2800-km SMF-28 with EDFA only," presented at the ECOC 2012, Amsterdam, Netherland, Sep. 15–20, 2012, paper Mo.2.C.2.
15. J. Li, M. Sjödin, M. Karlsson, and P. A. Andrekson, "Building up low-complexity spectrally-efficient Terabit superchannels by receiver-side duobinary shaping," Opt. Express **20**(9), 10271–10282 (2012).
16. H. Wang, J. Li, D. Kong, Y. Li, W. Li, J. Wu, K. Xu, and J. Lin, "Multi-carrier group detection in receiver-side duobinary-shaped WDM superchannel systems," IEEE Photon. Technol. Lett. **24**(14), 1206–1208 (2012).
17. J. Li, M. Karlsson, and P. A. Andrekson, "1.94Tb/s (11×176Gb/s) DP-16QAM superchannel transmission over 640 km EDFA-only SSMF and two 280GHz WSSs," presented at ECOC2012, Amsterdam, Netherland, Sep. 2012, paper Th.2.C.1.
18. P. J. Winzer, and A. H. Gnauck, "112-Gb/s polarization-multiplexed 16-QAM on a 25-GHz WDM grid," presented at ECOC2008, Brussels, Belgium, Sep. 2008, paper Th.3.E.5.
19. A. H. Gnauck, P. J. Winzer, C. R. Doerr, and L. L. Bu, "10x112-Gb/s PDM 16-QAM transmission over 630km of fiber with 6.2-b/s/Hz spectral efficiency," presented at OFC2009, San Diego, CA, Mar. 2009, paper PDPB8.
20. M. S. Alfiad, M. Kuschnerov, S. L. Jansen, T. Wuth, D. van den Borne, and H. de Waardt, "11×224-Gb/s POLMUX-RZ-16QAM transmission over 670 km of SSMF with 50-GHz channel spacing," IEEE Photon. Technol. Lett. **22**(15), 1150–1152 (2010).
21. M. Selmi, Y. Jaouën, and P. Ciblat, "Accurate digital frequency offset estimator for coherent PolMux QAM transmission systems," in Proc. ECOC 2009, Sep. 2009, Paper P3.08.
22. J. Li, L. Li, Z. Tao, T. Hoshida, and J. C. Rasmussen, "Laser-linewidth- tolerant feed-forward carrier phase estimator with reduced complexity for QAM," J. Lightwave Technol. **29**(16), 2358–2364 (2011).
23. M. Scholten, T. Coe, and J. Dillard, "Continuously-interleaved BCH (CI-BCH) FEC delivers best in class NECG for 40G and 100G metro applications," presented at OFC2010, San Diego, CA, Mar. 2010, paper NTuB3.

1. Introduction

The increase of both the per-channel data rate and the spectral efficiency promises to reduce the cost per bit and to scale up the capacity, which has motivated intense research on spectrally-efficient optical transmission systems beyond 100G [1–8]. The highest per-channel transport rate today is 112 Gb/s which can carry one 100 Gb/s Ethernet payload. Since the next Ethernet rate will likely be 400 Gb/s, 1.6 Tb/s will be a reasonable follow-on rate in an investment perspective [9]. In order to accommodate one 1.6 Tb/s Ethernet payload, the channel rate needs to be scaled up to >1.92 Tb/s, which reserves 20% overhead for future advanced forward error correction (FEC). Multi-carrier-based superchannels have been proposed to address the challenges at such high channel rate in the form of orthogonal frequency-division multiplexing (OFDM) [2–4], Nyquist wavelength-division multiplexing (WDM) [5–7], and sub-Nyquist WDM [8]. More recently, we proposed a low-complexity receiver-side digital spectral shaping technique [10,11] to achieve comparable spectral efficiencies w.r.t. sub-Nyquist WDM. It enables smooth upgrading capability from the commercial 100G WDM systems by narrowing the channel spacing [10,11,13] or increasing the symbol rate [12, 14]. Like OFDM and Nyquist-WDM, the proposed technique has also been proposed to build up multi-carrier superchannels beyond 100G [15]. In addition, multi-carrier group detection was experimentally demonstrated to show the potential of sampling efficiency enhancement and cost reduction [16].

In the most of the previous demonstrations [10, 12–16], the modulation format of dual-polarization quadrature phase-shift keying (DP-QPSK) was exclusively applied. In [11], we attempted to extend the proposed receiver-side spectral shaping technique for dual-polarization 16-ary quadrature amplitude modulation (DP-16QAM), where duobinary was remained as the intermediate response without any optimization. As is well known, DP-16QAM exhibits lower tolerance to the noise and the linear crosstalk than DP-QPSK does. Therefore, the symbol rate is commonly set below the carrier spacing for DP-16QAM to avoid significant narrowband filtering and linear crosstalk. In this case, duobinary would not be a good choice as the intermediate response. In [17], we introduced a parameter α in the transfer function of the intermediate response to offer one degree of optimization freedom while maintaining the minimal state count of the maximum-likelihood sequence detection (MLSD). Transmission of 1.936 Tb/s 11-carrier DP-16QAM superchannels was achieved over 8 × 80 km standard single-mode fiber (SSMF) with Erbium-doped fiber amplifiers (EDFAs) only and two wavelength selective switches (WSSs). The total bit rate of 1.936Tb/s can support potential 1.6T Ethernet service allowing ~20% soft-decision-based FEC

#177331 - $15.00 USD Received 1 Oct 2012; revised 11 Nov 2012; accepted 11 Nov 2012; published 29 Nov 2012

overhead. However, due to the limited experimental environment, the transmission line in the demonstration is only 640 km long (i.e. 8 × 80 km), which leads to a bit-error rate (BER) below the threshold of the state-of-the-art 7%-overhead hard-decision FEC. Therefore, the transmission reach can be extended by applying ~20%-overhead soft-decision FEC and soft-output MLSD. In this paper, we provide more details of the principle and the experimental results, as compared to [17].

2. Optimization of the intermediate response for DP-16QAM

In the prior investigations using DP-QPSK format [10–16], the symbol rate can be pushed above the carrier/channel spacing to enable the so-called faster-than-Nyquist or sub-Nyquist operation. For example, the symbol rate can go up to 32 Gbaud given a carrier/channel spacing of 25 GHz [13]. However, the case is different for DP-16QAM format which is less tolerant to noise and linear crosstalk. For DP-16QAM, the same amount of narrowband filtering and linear crosstalk might destroy the convergence of the blind adaptive equalization due to the noise and crosstalk enhancement, which disables the following digital signal processing (DSP). Therefore, we need to make a compromise on the spectral efficiency. In this paper, the symbol rate is reduced to 22 Gbaud given a carrier spacing of 25 GHz for DP-16QAM. Note that the 22 Gbaud line-side symbol rate is not compatible with the next client-side electrical interface rate (e.g. 25 Gb/s), which will necessitate gear-boxes for adaptation in real implementation. One alternative option is to keep the compatibility to the client-side interface rate while slightly increasing the given 25 GHz carrier spacing. The optical spectra of the 28 Gbaud DP-QPSK and 22 Gbaud DP-16QAM signals are shown in Fig. 1 together with the transmission function of a commercial 25/50 GHz interleaver. It can be observed that the 22 Gbaud DP-16QAM experiences lower degree of narrowband filtering as compared to 28 Gbaud DP-QPSK. The next concern is what will happen with relaxed narrowband filtering.

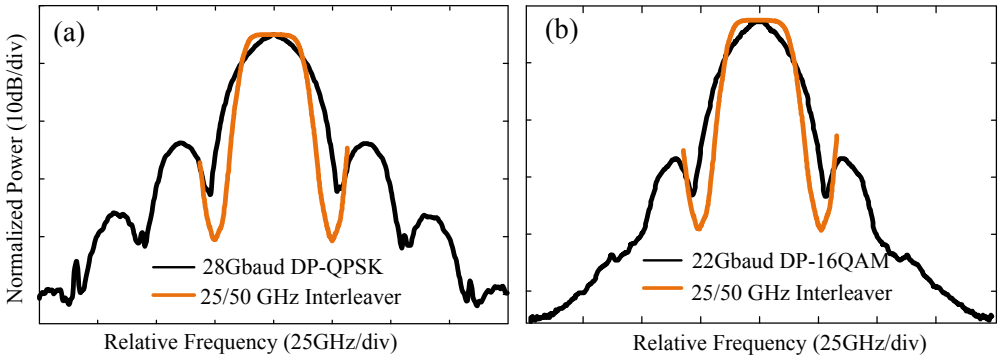

Fig. 1. The optical spectra of (a) 28 Gbaud DP-QPSK and (b) 22 Gbaud DP-16QAM, together with the transmission function of a commercial 25GHz/50GHz interleaver.

As explained in [11], an intermediate response needs to be determined while implementing the proposed receiver-side spectral shaping. The selection criterion is that the intermediate response is close to the actual channel response as much as possible. In the previous demonstrations using DP-QPSK under sub-Nyquist operation [10–16], duobinary was selected as the intermediate response which has a transfer function in z-transform of $H(z) = 1 + z^{-1}$. In [17], we introduced a tap coefficient α ($0 \le \alpha \le 1$) to facilitate the optimization of the intermediate response case by case while keeping the same one-symbol channel memory. The equivalent amplitude responses of the intermediate response $H(z) = 1 + \alpha z^{-1}$ are shown in Fig. 2(a) for different values of α. Figure 2(b) shows the performance penalty as a function of the value of α for 28 Gbaud DP-QPSK and 22 Gbaud DP-16QAM in a 25 GHz WDM grid (the transmitter-side narrowband filtering is done by a commercial 25/50 GHz optical interleaver). It can be seen that $\alpha = 1$ (i.e. duobinary) gives the optimum for DP-QPSK. In

#177331 - $15.00 USD Received 1 Oct 2012; revised 11 Nov 2012; accepted 11 Nov 2012; published 29 Nov 2012

contrast, the optimal value of α is ~0.4 for DP-16QAM since the symbol rate is reduced to 22 Gbaud given the same WDM grid (i.e. 25 GHz). Note that the case with $\alpha = 0$ is equivalent to the hard decision since no digital spectral shaping was done and the MLSD didn't have any memory to use. Therefore, it is beneficial to optimize the value of α for different spectral efficiencies.

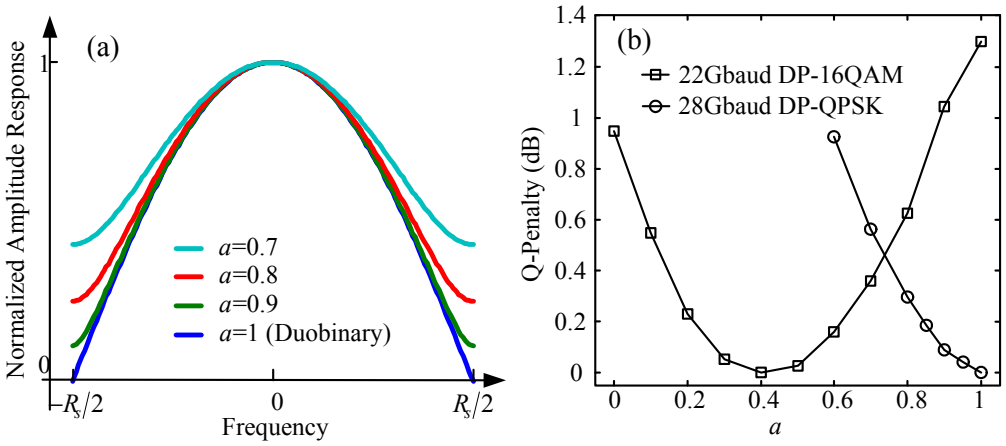

Fig. 2. (a) The equivalent amplitude responses of $H(z) = 1 + \alpha z^{-1}$; (b) Q-penalty as a function of α.

3. Experimental setup and DSP algorithms

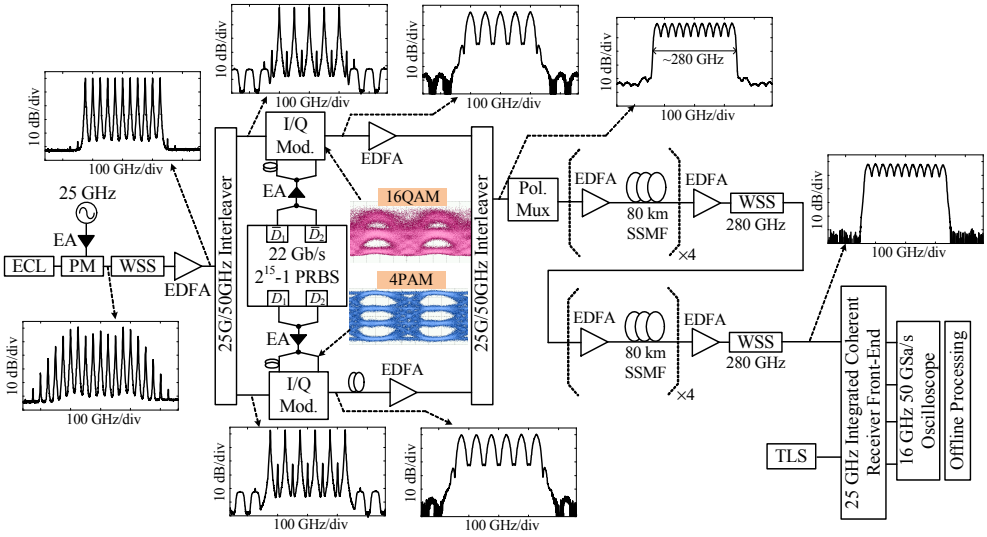

Fig. 3. Experimental setup, optical spectra and eye diagrams. EA: electrical amplifier

The experimental setup, the optical spectra and eye diagrams are shown in Fig. 3. The super-channel under study consists of eleven 25 GHz-spaced carriers each of which carries a 176 Gbit/s DP-16QAM signal. The 11 carriers were generated from a single external-cavity laser (ECL) with ~100 kHz linewidth at 1598.89 nm by using one phase modulator (PM) (Vpi≈4V). The PM was driven by a boosted 25 GHz clock signal with a peak-to-peak voltage of ~17 V. After the PM, >15 carriers were produced, and the central 11 carriers were selected and gain-equalized by a WSS (i.e. Finisar WaveShaper). After gain equalization, the power difference kept within 0.3 dB. These 11 carriers were separated to even and odd groups by a

#177331 - $15.00 USD Received 1 Oct 2012; revised 11 Nov 2012; accepted 11 Nov 2012; published 29 Nov 2012

25/50 GHz optical interleaver. Two I/Q modulators driven by two pairs of decorrelated 4-ary pulse amplitude modulation (4PAM) signals were used to obtain 22 Gbaud optical 16QAM signals. Each 4PAM driving signal with ~1.9 V_{pp} was derived from two decorrelated 2^{15}-1 pseudo-random bit sequence (PRBS) signals with different amplitudes by combining, linear amplifying and splitting [18–20]. The amplitude difference of the two PRBS signals was optimized to take into account the modulation nonlinearity. The differential delays were 2^{14} bits between PRBS data D_1 and D_2, and 43 symbols between the two 4PAM signals in I and Q paths. After the even and odd decorrelation by optical delay lines, the 22 Gbaud 16QAM signals in even and odd carriers were strongly-filtered and combined together by another 25/50 GHz optical interleaver. After polarization multiplexing, the 11-carrier superchannel signal was launched into a 8 × 80 km EDFA-only SSMF link containing two WSSs with a 3-dB bandwidth of 280 GHz. Coherent detection of the eleven carriers was implemented one by one through a commercial integrated coherent receiver. The central wavelength of the tunable laser source (TLS) with ~100 kHz linewidth was tuned to determine which carrier was detected. Finally, the detected electrical signals were digitized and captured with 5 × 10^6 samples each by a 50 GSa/s digital sampling oscilloscope with a 16 GHz analog bandwidth for offline processing.

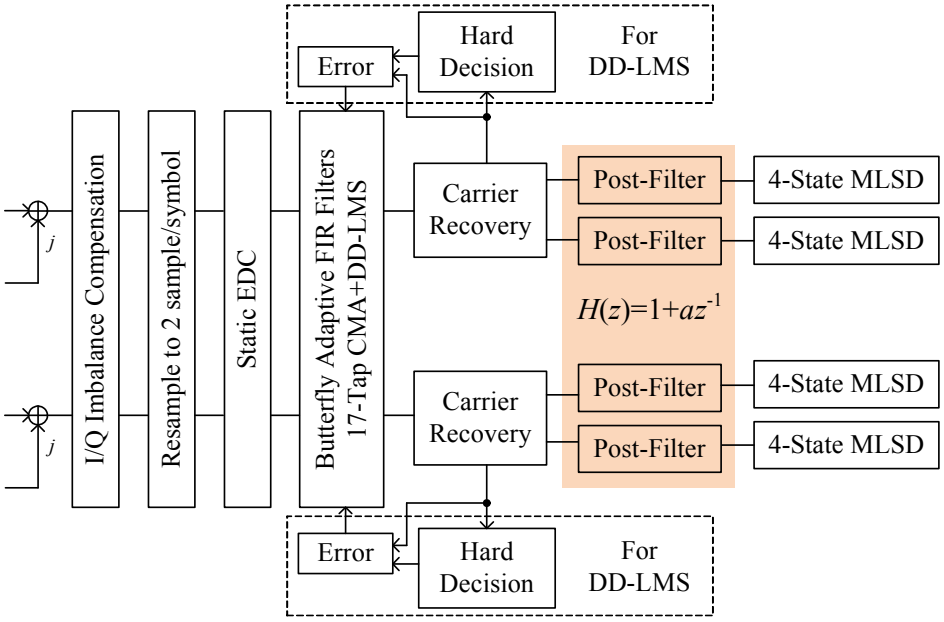

Fig. 4. offline DSP flow.

The offline DSP flow is shown in Fig. 4. The details of the DSP algorithms can be found in [11]. After I/Q imbalance compensation, the four sample streams were resampled to 2 samples/symbol. The electronic dispersion compensation (EDC) was next performed to compensate for the accumulated dispersion in the fiber link. The adaptive equalization and polarization demultiplexing were performed by four butterfly 21-tap *T*/2-spaced finite impulse-response (FIR) filters. These FIR filters were first adapted by the standard constant-modulus algorithm (CMA) for pre-convergence. Final adaptation was done by switching CMA to decision-directed least-mean-square (DD-LMS). In the DD loop, the carrier recovery included frequency offset estimation based on the fast Fourier transform (FFT) method [21] and the carrier phase estimation based on the improved blind phase search method [22]. It is worth emphasizing here that the DD-LMS was based on the hard decision instead of MLSD, which enables independent implementation of the typical DSP functions and the newly proposed ones (i.e. the post-filter and MLSD). From a practical point of view, this helps to reduce the decision-directed loop delay, accelerate the filter convergence, and facilitate DSP

#177331 - $15.00 USD Received 1 Oct 2012; revised 11 Nov 2012; accepted 11 Nov 2012; published 29 Nov 2012

reconfiguration (i.e. the post-filter and the MLSD can be easily switched to the hard decision). The spectral-shaping post-filter in the form of $H(z) = 1 + \alpha z^{-1}$ and corresponding MLSD were implemented on each individual signal quadrature path of each polarization where the signal can be considered as a spectrally-shaped 4PAM. The tap coefficient α was optimized.

4. Experimental results

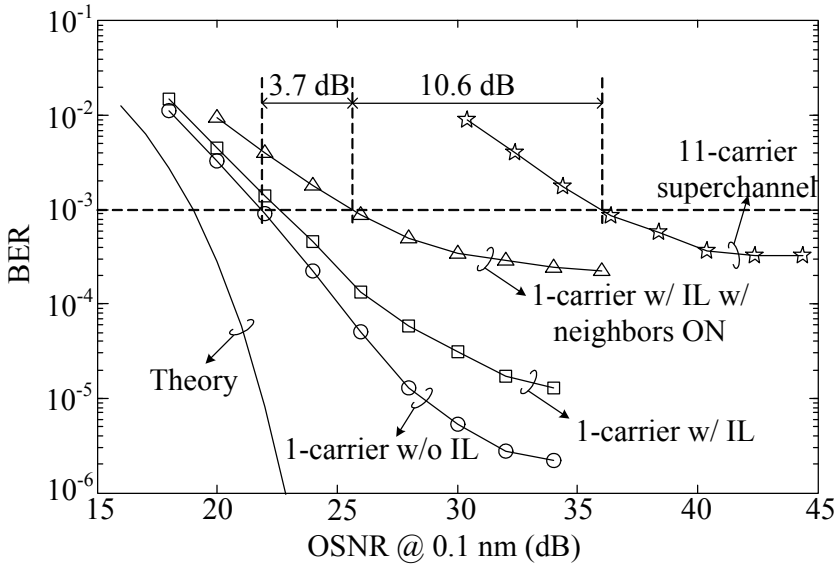

Fig. 5. BER performance at B2B.

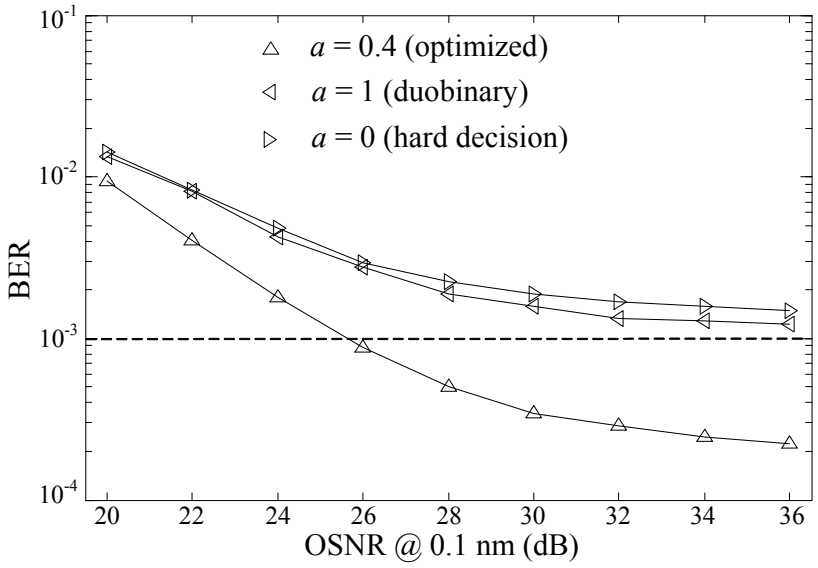

Fig. 6. B2B performance for different α.

The B2B results are shown in Fig. 5. Firstly, the performance of single-carrier 22 Gbaud DP-16QAM without interleaver was measured. Since there is no pre-filtering, the post-filter and MLSD were replaced by the conventional hard decision. As compared to the theory, there is

#177331 - $15.00 USD Received 1 Oct 2012; revised 11 Nov 2012; accepted 11 Nov 2012; published 29 Nov 2012

<3 dB implementation penalty at BER = 10^{-3}. Secondly, the 25/50 GHz interleaver was inserted. In this case, the post-filter and MLSD were activated. The tap coefficient α was optimized to minimize the BER. It can be seen that the insertion of the 25/50 GHz interleaver brought <1dB optical signal-to-noise ratio (OSNR) penalty at BER = 10^{-3}.Thirdly, we turned on the two adjacent carriers around the carrier under study. In this case, the optimal α is 0.4, as shown in Fig. 2(b). With the optimal α, there is ~3.7 dB OSNR penalty at BER = 10^{-3} in the presence of both the pre-filtering and linear crosstalk. For the entire 11-carrier superchannel (stars in Fig. 5), the required OSNR at BER = 10^{-3} is 10.6 dB higher than that of the single-carrier with two neighbors ON (triangles in Fig. 5), showing negligible excess penalty during the formation of the superchannel. The performance at B2B for three typical α is shown in Fig. 6. Note that the case with $\alpha = 0$ is equivalent to the hard decision since no spectral shaping was done and the MLSD didn't have any memory to use. It can be seen that the optimization of α brought dramatic performance improvement. This is because the filtering profile of the commercial 25/50 GHz interleaver is broad w.r.t. the 22 Gbaud 16QAM signal, and the duobinary is no more suitable as the target of the receiver-side spectral-shaping. For both cases with the duobinary shaping and the hard decision, the BER is unable to reach 10^{-3}.

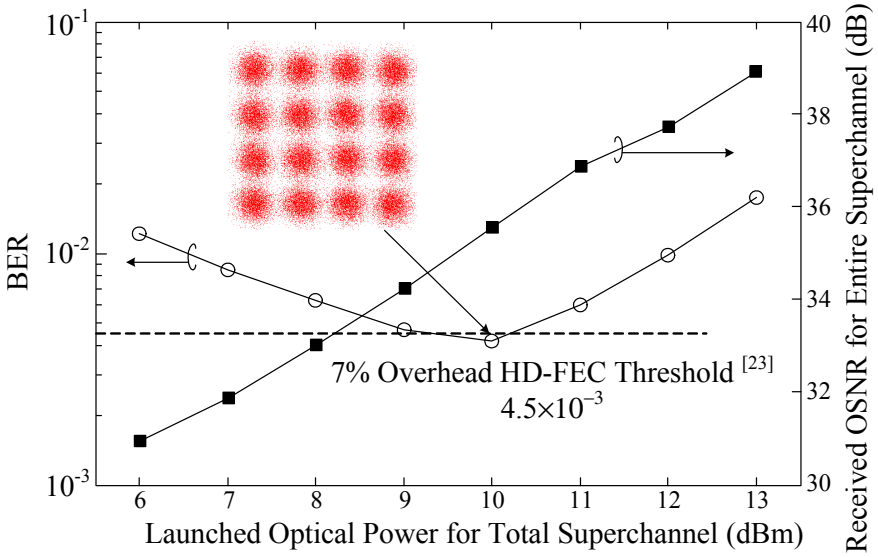

Fig. 7. Performance after fiber transmission.

Figure 7 shows the average BER of entire 11-carrier superchannel after 640 km transmission with two WSSs and the corresponding received OSNR as a function of the launched optical power to the fiber. At optimal launched power, there is a large margin as compared to the FEC threshold with 20% overhead, and the BER is even below the hard-decision FEC (HD-FEC) threshold with 7% overhead [23]. Figure 7 also shows the recovered constellation of the central carrier before the spectral-shaping post-filter. In Fig. 8, we show the optical spectra of the superchannel before and after transmission and BERs of all 11 carriers, as well as the measured passband of the two cascaded 280 GHz WSSs. Note that the two outer carriers subject to one-sided linear crosstalk have lower BERs. It was found that there was no performance loss for the two outer carriers after passing through 2 concatenated 280 GHz WSSs. The Q-penalties of 1st and 11th carriers as a function of the 3-dB bandwidth of WSSs are plotted in Fig. 9. Note that the narrowband filtering effect induced by the concatenation of multiple WSSs mainly influence the most outer two carriers (i.e. 1st and 11th carriers). Given a Q-penalty within 1 dB, the two carriers can tolerant a 3-dB WSS

#177331 - $15.00 USD Received 1 Oct 2012; revised 11 Nov 2012; accepted 11 Nov 2012; published 29 Nov 2012

bandwidth of as low as 270 GHz. This means the 1.934 Tb/s superchannel signal can be well fit into a 300GHz WSS channel with sufficient guardband.

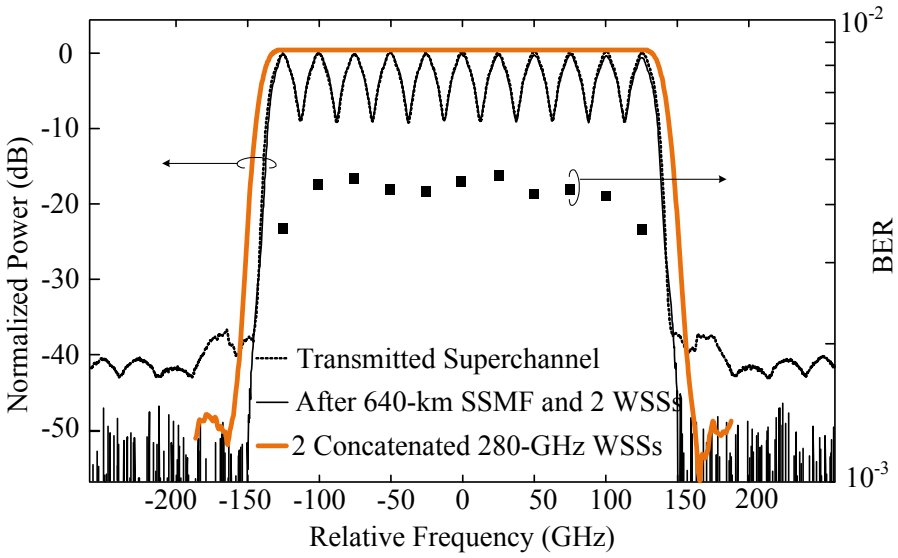

Fig. 8. Optical spectra and BERs for 11 carriers after transmission.

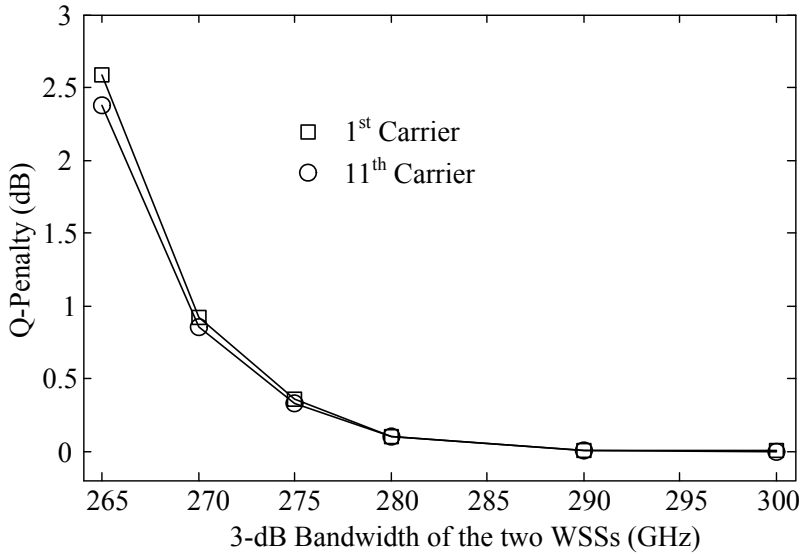

Fig. 9. Optical spectra and BERs for 11 carriers after transmission.

5. Conclusion

DP-16QAM is less tolerant to the noise and linear crosstalk as compared to DP-QPSK. Consequently, the symbol rate has to be reduced below the carrier spacing for DP-16QAM to avoid significant narrowband filtering and linear crosstalk. If we continue to apply the proposed receiver-side spectral shaping technique in DP-16QAM superchannel systems, the intermediate response needs to be optimized. By introducing one tap coefficient α, we can have one degree of freedom to optimize the intermediate response while maintaining the same one-symbol memory and the state count of MLSD. With the improved receiver-side spectral

#177331 - $15.00 USD Received 1 Oct 2012; revised 11 Nov 2012; accepted 11 Nov 2012; published 29 Nov 2012

shaping technique, we have experimentally demonstrated 1.936 Tb/s DP-16QAM superchannel transmissions over 640 km SSMF with EDFA-only and 300 GHz WSS channel with sufficient guardband. The transmission reach can be further increased by employing advanced FEC with ~20% overhead.

Acknowledgment

This work was supported in part by 863 Program in China (2011AA010306, 2011AA010305), the Swedish Foundation for Strategic Research (SSF), and Beijing Excellent Doctoral Thesis Project under Grant YB20101001301.

#177331 - $15.00 USD Received 1 Oct 2012; revised 11 Nov 2012; accepted 11 Nov 2012; published 29 Nov 2012